Phytochemistry 159 (2019) 208–215

Contents lists available at ScienceDirect

Phytochemistry

journal homepage: www.elsevier.com/locate/phytochem

A phytochemical investigation of *Stemona parviflora* roots reveals several compounds with nematocidal activity

Sheng-Zhuo Huang[a], Fan-Dong Kong[a], Gao Chen[b], Xiang-Hai Cai[b], Li-Man Zhou[a], Qing-Yun Ma[a], Qi Wang[a], Wen-Li Mei[a], Hao-Fu Dai[a,*], You-Xing Zhao[a,**]

[a] Hainan Key Laboratory for Research and Development of Natural Products from Li Folk Medicine, Institute of Tropical Bioscience and Biotechnology, Chinese Academy of Tropical Agriculture Sciences, Haikou 571101, China

[b] Yunnan Key Laboratory for Integrative Conservation of Plant Species with Extremely Small Populations, Kunming Institute of Botany, Chinese Academy of Sciences, Kunming, 650204, China

ARTICLE INFO

Keywords:
Stemona parviflora
Stemonaceae
Phenanthrene
Stilbene
Nematocidal activity

ABSRACT

Twelve undescribed compounds including six phenanthrene derivatives (parviphenanthrines A-F), two stilbene derivatives (parvistilbines A-B), three esters (parviesters A-C), and one sesquiterpenoid (parvidiol A) were isolated from the roots of *Stemona parviflora*, together with twenty-two known ones. The structures of the undescribed compounds were elucidated based on the analyses of their spectroscopic data. The absolute configuration of parviphenanthrine A was determined by the quantum ECD calculations. Parviphenanthrines A and E, stemanthrene A, stilbostenin E, 4-hydroxy-benzenepropanol-*α*-benzoate, and (*E*)-4-hydroxycinnamic acid methyl ester showed nematocidal activity against *Meloidogyne incognita* with IC_{50} values of 14.02 ± 0.32, 2.51 ± 0.13, 17.10 ± 0.65, 2.05 ± 0.07, 4.22 ± 0.31, and 1.07 ± 0.05 μM, respectively.

1. Introduction

Plant-parasitic nematodes, common pathogens, have impaired a wide range of agriculture and forestry land worldwide (Bird and Kaloshian, 2003). The root-knot nematodes (*Meloidogyne* spp. a series of pathogenic nematodes), are causing uncontrollable loss to worldwide annual global crop production (Bird and Kaloshian, 2003). They can infect and damage crop roots, which impedes water and nutrient absorption and leads to phytopathogen infections (Yu, 1999). Therefore, a chemical nemacide with high efficiency and low toxicity is needed in controlling plant-parasitic nematodes as a key to protect plant roots and prevent phytopathogenic infections (Oka et al., 2009).

Chinese medicine herbs have a long history in botanic protection, and some *Stemona* roots have been used for killing agricultural insect for thousand years. Three *Stemona* species [*S. tuberosa* L., *S. japonica* (Blume) Miquel, and *S. sessilifolia* Miquel.] from the Stemonaceae family are listed as pesticidal in the Chinese Pharmacopoeia (Commission of China Pharmacopoeia, 2015). Alternatively, the similar fleshy tuberous roots of *Stemona parviflora* C. H. Wright (Stemonaceae family) are also used by the Li ethnic group as an agricultural industry pesticide in Hainan Island (Dai, 2010). Nowadays, the *Aquilaria sinesis* germ chits were in danger of root-knot nematodes in Hainan province. And then people are paying more attention to the organic eaglewood with high quality. So a safety and low mammalian toxicity nemacide eaglewood was needed in *A. sinesis* planting industry. In addition to previous finding that the alkaloids from *S. parviflora* have moderate nematocide activities (Huang et al., 2016; Xing et al., 2014), the non-alkaloid extract in our preliminary experiment also showed good anti-nematode activity with 76.21 ± 2.43% RDR (250 μg/mL). To verify the preliminary results, we performed a phytochemical investigation of the non-alkaloid extract with twelve undescribed and twenty-two known compounds were isolated from *S. parviflora* root and anti-nematode bioassays of the isolated compounds (see Fig. 1).

2. Results and discussion

Compound **1** was purified as a white crystal, and its molecular formula was assigned as $C_{17}H_{18}O_4$, with nine degrees of unsaturation, from its positive HREIMS (*m/z* 309.1105 $[M+Na]^+$, calcd for $C_{17}H_{18}O_4Na$, 309.1103) and NMR spectroscopic data (Table 1). The IR spectrum displayed bands for the presence of hydroxy (3416 cm^{-1}), carbonyl (1662 cm^{-1}) and double bonds (1573 and 1484 cm^{-1}). Analysis of the ^{13}C NMR spectra and DEPT spectra (Table 1) showed 17 carbon resonances, including these for three methyls (two methoxys),

* Corresponding author.
** Corresponding author.
E-mail addresses: daihaofu@itbb.org.cn (H.-F. Dai), zhaoyouxing@itbb.org.cn (Y.-X. Zhao).

https://doi.org/10.1016/j.phytochem.2018.12.021
Received 21 August 2018; Received in revised form 24 December 2018; Accepted 27 December 2018
Available online 08 January 2019
0031-9422/

Table 1
^{1}H (500 MHz) and ^{13}C NMR (125 MHz) data of 1–6 (in $CDCl_3$).

No.	1		2		3		4		5		6	
	δ_H mult. (*J* in Hz)	δ_C	δ_H mult. (*J* in Hz)	δ_C	δ_H mult. (*J* in Hz)	δ_C	δ_H mult. (*J* in Hz)	δ_C	δ_H mult. (*J* in Hz)	δ_C	δ_H mult. (*J* in Hz)	δ_C
1		143.8 s		139.7 s		143.6 s		143.5 s		143.4 s		144.9 s
2		147.4 s		147.6 s		146.9 s		147.0 s		146.8 s		150.9 s
3	6.89 d (9.0)	114.2 d	9.32 d (9.0)	126.3 d	7.83 d (8.6)	112.9 d	6.90 d (8.6)	113.1 d	6.89 d (8.7)	112.5 d	6.84 d (8.8)	109.7 d
4	7.80 d (9.0)	126.0 d	7.44 d (9.0)	121.2 d	6.75 d (8.6)	124.4 d	8.09 d (8.6)	124.1 d	7.95 d (8.7)	124.9 d	8.09 d (8.8)	123.4 d
4a		130.3 s		128.1 s		125.9 s		126.3 s		126.0 s		126.9 s
4b		51.9 s		140.4 s		115.5 s		120.0 s		140.4 s		120.1 s
5		203.1 s		156.8 s		157.7 s		118.6 s	6.46 d (2.2)	104.7 d		154.6 s
6	5.48 d (2.0)	98.3 d		125.5 s	6.36 d (2.0)	98.0 d		156.9 s		158.8 s		114.8 s
7		170.7 s		189.1 s		155.9 s		156.1 s	6.49 d (2.3)	97.5 d		151.4 s
8	6.02 d (2.0)	115.0 d		181.9 s	6.31 d (2.0)	107.1 d		106.1 d		157.6 s		116.2 s
8a		159.5 s		132.6 s		140.6 s		130.8 s		116.7 s		136.7 s
9	3.26 m	26.6 t	8.18 d (8.8)	122.3 d	2.73 m	30.0 t	2.75 m	30.0 t	2.75 m	30.3 t	2.70 m	21.8 t
10	2.67 m	30.2 t	8.28 d (8.8)	126.0 d	2.16 m	22.1 t	2.84 m	22.4 t	2.83 m	22.3 t	2.83 m	25.7 t
10a		130.0 s		131.8 s		131.3 s		137.1 s		130.9 s		131.8 s
1-sub	3.73 s	61.4 q			3.86 s	60.8 q	3.84 s	61.4 q	3.80 s	61.4 q	3.86 s	60.8 q
2-sub			3.99 s	62.1 q							3.93 s	55.7 q
5-sub			4.14 s	61.0 q	3.79 s	55.3 q	2.22 s	8.9 q			3.53 s	60.0 q
6-sub			2.15 s	9.6 q			3.56 s	59.6 q	3.89 s	56.5 q	2.27 s	8.9 q
7-sub	3.74 s	56.7 q					3.88 s	56.6 q				
8-sub									3.87 s	56.3 q	2.24 s	11.8 q
4b-sub	1.64 s	32.7 q										

two methylenes, four olefinic methines, and eight quaternary carbons (one carbonyl and six olefinic). The ^{13}C NMR spectroscopic partial data of **1** was similar to those of stemanthrene B (**14**) (Kostecki et al., 2004), except for the ring resonances at δ_C 51.9 (s, C-4b), 203.1 (s, C-5), 98.3 (s, C-6), 170.7 (s, C-7), 115.0 (d, C-8), and 159.5 (q, C-8a) and methyl resonance at δ_C 32.7 (q, methyl-4b), replacing benzene ring resonances at δ_C 115.5 (s, C-4b), 156.4 (s, C-5), 117.2 (d, C-6), 151.7 (s, C-7), 102.8 (d, C-8), and 131.9 (q, C-8a) and methyl resonance at δ_C 55.6 (q, 6-methyl) in stemanthrene B, indicating that the benzene ring was oxygenated with a carbonyl at C-5 and the methyl group was linked at C-4b, but not at C-6 in compound **1**. This deduction was verified by the ^{1}H ^{1}H COSY cross-peaks and HMBC (Fig. 2) correlations observed for **1**. The sequential ^{1}H ^{1}H COSY cross-peaks of H-3 [δ_H 6.89 (1H, d, J = 9.0 Hz)]/H-4 [δ_H 7.80 (1H, d, J = 9.0 Hz)] and H-9 [δ_H 3.26 (2H, m)]/H-10 [δ_H 2.67 (2H, m)] confirmed the linkages of C-3-C-4 and C-9-C-10, respectively. The HMBC (Fig. 2) correlations from H-6 [δ_H 5.48 (1H, d, J = 2.0 Hz)] to C-4b, C-5 and C-7 and from H-methyl-4b [δ_H 1.64 (3H, s)] to C-4a [δ_C 130.3 (s)], C-4b, C-5, and C-8a supported the connectivities of compound **1** as shown in Fig. 2. The other HMBC correlations further confirmed the atom connectivity in compound **1**. The *R* configuration of the only stereogenic center (C-4b) in compound **1** was proposed from ECD calculations (Fig. 3) using the time-dependent density functional theory (TD-DFT) method at the B3LYP/6-31G(d) level as implemented in the Gaussian 03 program package (Stephens et al., 2007). The ECD calculations were performed after optimization of the selected conformers at the B3LYP/6-31G(d) levels (Huang et al., 2016). The calculated ECD curve for (*R*)-**1** matched well with the experimental one. Thus, the structure of compound **1** was assigned as shown and named as parviphenanthrine A.

Compound **2** was isolated as a colorless solid and the ESIMS *m/z* 321 $[M+Na]^+$ suggested its molecular weight to be 298 Da. The molecular formula of **2** was determined as $C_{17}H_{14}O_5$ with eleven degrees of unsaturation by negative HRESIMS (*m/z* 297.0771 $[M-H]^-$, calcd for $C_{17}H_{13}O_5$, 297.0763). Analysis of the NMR spectroscopic data (Table 1) showed compound **2** also had the phenanthrene skeleton as stemanthrene B (**14**) (Kostecki et al., 2004). The significant NMR differences between compound **2** and stemanthrene B were the resonances at δ_C 140.4 (s, C-4b), 156.8 (s, C-5), 125.5 (s, C-6), 189.1 (s, C-7), 181.9 (d, C-8), 132.6 (s, C-8a), 122.3 (d, C-9), and 126.0 (d, C-10) in compound **2** replacing the resonances at δ_C 115.5 (s, C-4b), 156.4 (s, C-5), 117.2 (d, C-6), 151.7 (s, C-7), 102.8 (d, C-8), 131.9 (q, C-8a), 22.7 (t, C-9), and 30.0 (t, C-10) in stemanthrene B, indicating that the benzene ring was oxygenated with carbonyls at C-7 and C-8, and the linkage of C-9-C-10 was dehydrogenated to a double bond in compound **2**. The key HMBC correlations from H-9 [δ_H 8.18 (1H, d, J = 8.8 Hz)] to C-4b, C-8, and C-8a, and from H-6-methyl [δ_H 2.15 (3H, m)] to C-5, C-6, C-7, and the ^{1}H ^{1}H COSY correlations of compound **2** (Fig. 2) confirmed this supposition. Thus, the structure of compound **2** (parviphenanthrine B) was assigned as shown.

Compounds **3**, **4**, **5**, and **6** were isolated as separate compounds and formulated as $C_{16}H_{15}O_4$ (HRESIMS data at *m/z* 271.0976 $[M-H]^-$), $C_{18}H_{20}O_4$ (HRESIMS data at *m/z* 323.1255 $[M+Na]^+$), $C_{17}H_{18}O_4$ (HRESIMS data at *m/z* 309.1098 $[M+Na]^+$), and $C_{19}H_{21}O_4$ (HRESIMS data at *m/z* 313.1446 $[M-H]^-$), respectively. These four compounds had similar ^{13}C NMR spectroscopic data (Table 1) to those of stemanthrene B (**14**) in general (Kostecki et al., 2004), but differed in several points, this included loss of the 6-methy resonance (δ_C 8.8) in **3**, an added methoxy resonance [δ_C 56.6 (q, 7-OMe)] in **4**, added methoxy signal [δ_C 56.3 (q, 8-OMe)] and loss of the 6-methyl resonance (δ_C 8.8) in **5**, and added methyl (δ_C 11.8) and methoxy resonances [δ_C 55.7 (q, 2-OMe)] in **6**, respectively. These compounds **3–6** were derivatives of stemanthrene B with different substituents at C-2, C-5, C-6, C-7, and C-8. From the HMBC correlation analyses shown in Fig. 2, the different substituents from stemanthrene B were determined to be C-5-OMe, C-6-H, and C-7-OMe in compound **3**; C-5-Me and C-6-OMe in compound **4**, C-5-H, C-6-OMe, C-7-H, and C-8-OMe in compound **5**, and C-2-OMe, C-5-OMe, C-6-OMe, C-7-OH, and C-8-Me in compound **6**, respectively. Thus, the structures of compounds **3–6** (parviphenanthrines C-F) were assigned.

Compound **7**, was determined as $C_{18}H_{22}O_4$, with eight degrees of unsaturation, from HRESIMS (*m/z* 325.1409 $[M+Na]^+$, calcd for $C_{18}H_{22}O_4Na$, 325.1416. By comparing the molecular formula and NMR spectroscopic data (Table 2) of compound **7** with stilbostenin E (**18**) (Pacher et al., 2002), we proposed that compound **7** was derived from this stilbene via methylation at C-2′ and C-6′. The key HMBC correlations from H-2′-Me [δ_H 2.23 (3H, s)] to C-1′ [δ_C 140.7 (s)], C-2′ [δ_C 113.3 (s)], and C-3′ [δ_C 152.0 (s)], and from H-6′-Me [δ_H 2.22 (3H, s)] to C-1′, C-5′ [δ_C 156.3 (s)], and C-6′ [δ_C 116.9 (s)] in compound **7** (Fig. 2) supported the proposal. Thus, the structure of compound **7** (parvistilbine A) was assigned.

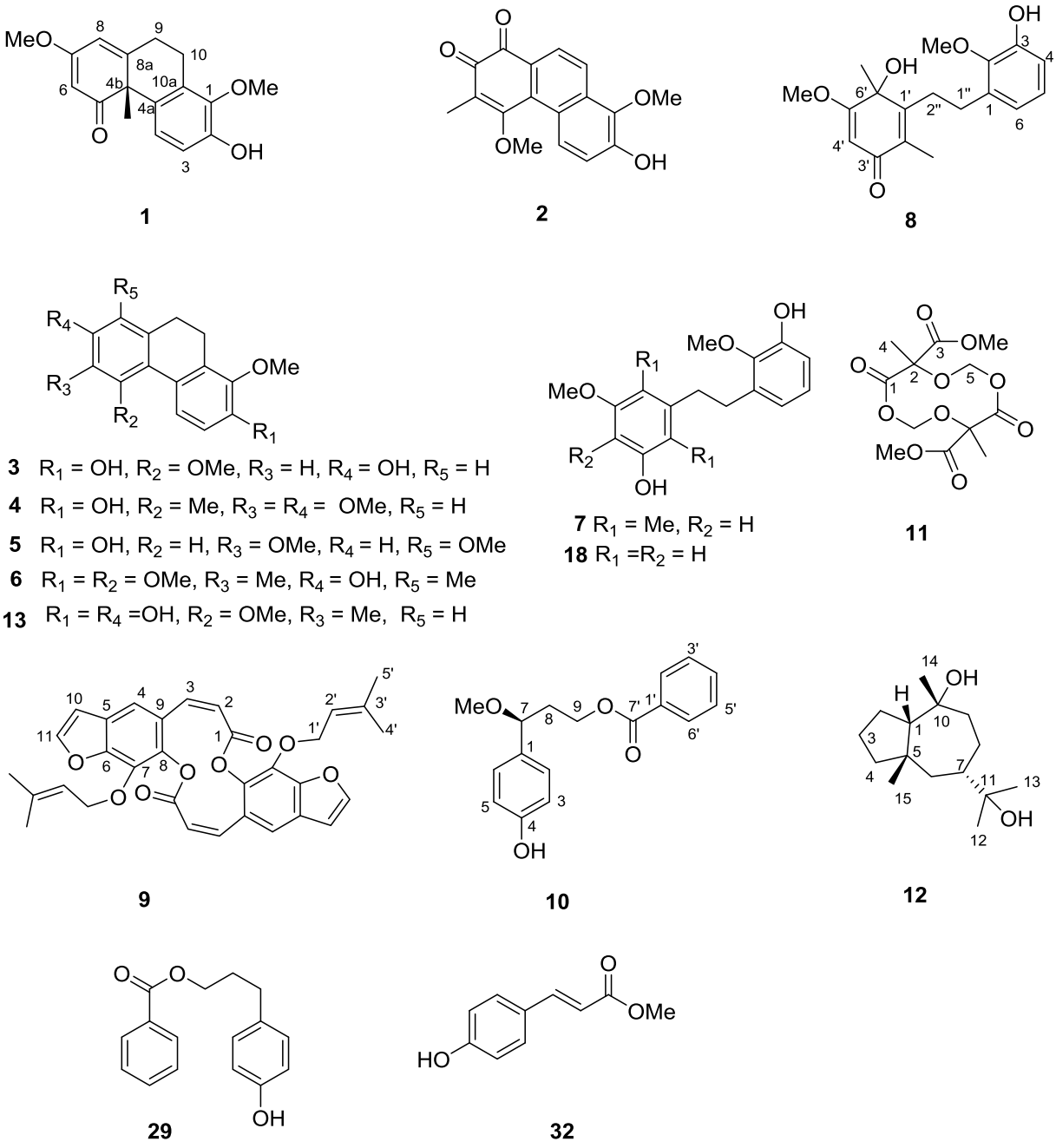

Fig. 1. Structures of **1–13**, **18**, **29**, and **32**.

Compound **8** was isolated as a colorless solid and the ESIMS *m/z* 341 $[M+Na]^+$ suggested its molecular weight to be 318 Da. The molecular formula of **8** was determined as $C_{18}H_{22}O_5$ by HRESIMS (*m/z* 341.1358 $[M+Na]^+$, calcd for $C_{18}H_{22}O_5Na$, 341.1356). By comparing the NMR spectroscopic data (Table 2) of compound **8** with those of compound **7**, we hypothesized that compound **8** was derived from this stilbene via oxygenation at C-3′ and C-6′ with generation of carbonyl and hydroxy groups, respectively. The key HMBC correlations from H-2′-Me [δ_H 2.00 (3H, s)] to C-1′ [δ_C 152.9 (s)], C-2′ [δ_C 130.6 (s)], and C-3′ [δ_C 187.0 (s)], and from H-6′-Me [δ_H 1.58 (3H, s)] to C-1′, C-5′ [δ_C 175.2 (s)], and C-6′ [δ_C 71.7 (s)] in compound **8** (Fig. 2) confirmed this hypothesis. The configuration of compound **8** was unable to be determined by 2D NMR data for the flexible link C-1″-C-2″. The structure of compound **8** (parvistilbine B) was assigned.

The molecular formula of compound **9** was determined to be $C_{32}H_{28}O_8$ with nineteen degrees of unsaturation from its HRESIMS (*m/z* 563.1676 $[M+Na]^+$, calcd for $C_{32}H_{28}O_8$, 563.1682). Compound **9** exhibited similar ^{13}C NMR spectroscopic data (Table 2) to those of 9-(isopentyloxy)-7*H*-furo [3,2-*g*] chromen-7-one (**24**) (Kalidhar, 1990), and their differences observed were the resonances at δ_C 119.8 (d, C-2′) and 139.8 (s, C-3′) in **9** replacing that at δ_C 40.3 (t, C-2′) and 23.4 (d, C-3′) in **24**. This indicated the compound **9** might be a derivative of **24** with olefination of C-2′-C-3′. The HMBC and ^1H ^1H COSY correlations of compound **9** (Fig. 2) supported this hypothesis. And according to formula of compound **9** ($C_{32}H_{28}O_8$) assigned by HRESIMS, the structure of compound **9** was verified to be a symmetrical cyclic ester as showed. Thus, the structure of compound **9** was assigned and named as parviester A.

Compound **10**, was determined as $C_{17}H_{18}O_4$, with nine degrees of unsaturation, from HRESIMS (*m/z* 309.1102 $[M+Na]^+$, calcd for $C_{17}H_{18}O_4Na$, 309.1103. By comparing the molecular formula and NMR spectroscopic data (Table 2) of compound **10** with 4-hydroxy-

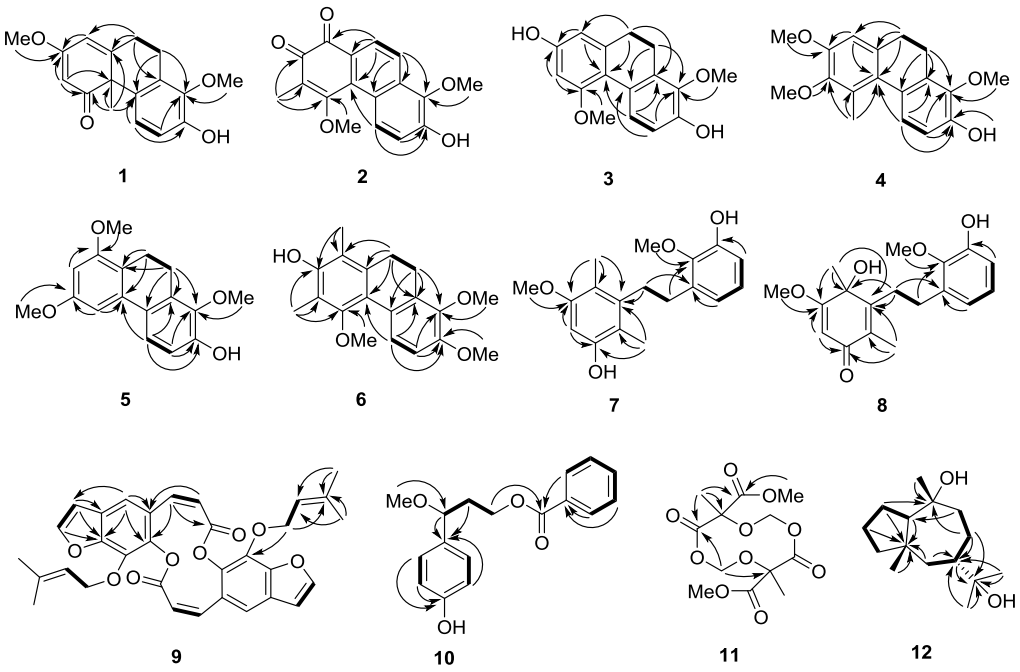

Fig. 2. Key HMBC (→) and ^{1}H ^{1}H COSY (━) correlations of **1–12**.

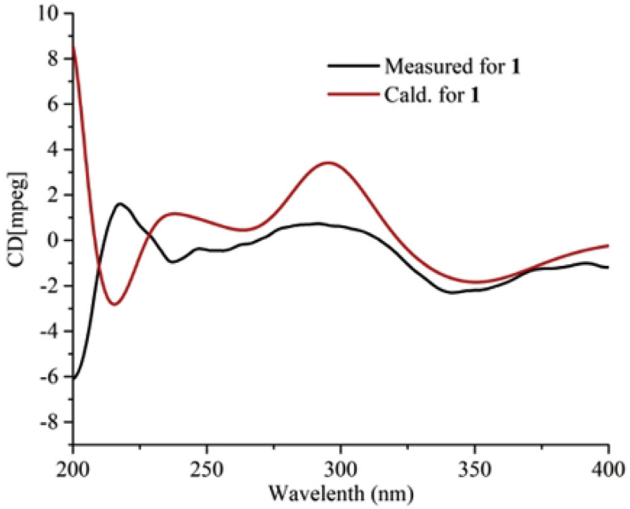

Fig. 3. Experimental and calculated ECD spectra for **1**.

benzenepropanol-*α*-benzoate (**29**) (Athikomkulchai et al., 2006), we proposed that compound **10** was derived from 4-hydroxy-benzenepropanol-*α*-benzoate via the methoxylation of C-7. A key HMBC correlation from H-7-OMe [δ_H 3.23 (3H, s)] to C-7 [δ_C 80.4 (d)] and ^{1}H ^{1}H COSY correlations between H-7/H-8 [δ_H 2.28 (1H, m) and 2.09 (1H, m)] and H-8/H-9 [δ_H 4.45 (1H, m) and 4.32 (1H, m)] in compound **10** (Fig. 2) supported the assignment. By comparing to 7,8-dihydro-(*R*)-7-methoxyconiferyl alcohol ([α]$_D$ = + 9.0) (Ngan et al., 2012), the configuration was assigned to 7*S* by the negative optical rotation value of compound **10** ([α]$_D$ = - 3.75). Thus, the structure of compound **10** (parviester B) was assigned as shown.

Compound **11**, was assigned to be $C_{12}H_{16}O_{10}$, with five degrees of unsaturation, from HRESIMS (*m/z* 319.0671 [M-H]$^-$, calcd for $C_{12}H_{15}O_{10}$, 319.0665). By analyzing the NMR data of compound **11**, we revealed three partial structures: a 2-hydroxy-2-methyl-malonic diester [δ_C 175.5 (s, C-1), 98.1 (s, C-2), 172.7 (s, C-3), and 6.8 (q, C-4)], a methylene [δ_C 65.6 (t, C-5)], and a methoxy group [δ_C 57.8 (q, -OMe)]. The 2-hydroxy-2-methyl-malonic diester part was verified by the HMBC correlations. The linkages of C-1-O-C-5-O-C-2 and C-3-OMe were confirmed by the key HMBC correlations (Fig. 2) from H-5 [δ_H 4.53 (m, 2H)] to C-1 and C-2 and from OMe-H [δ_H 3.86 (s, 3H)] to C-3, respectively. By analyzing the molecular formula $C_{12}H_{16}O_{10}$ proved by the HRESIMS, compound **11** was comprised two 2-hydroxy-2-methyl-malonic esters coupled through two methylene groups, probably derived from formaldehyde. Thus, the structure of compound **11** (parviester C) was assigned as shown.

The molecular formula of compound **12** was assigned as $C_{15}H_{28}O_2$, with two degrees of unsaturation, by its HREIMS (*m/z* 263.1980 [M + Na]$^+$, calcd for $C_{15}H_{28}O_2$, 263.1987). The ^{13}C NMR spectroscopic data of compound **12** were closely comparable to those of ambrosanoli-10, 11-diol (Vieira et al., 2010), except for some small differences in chemical shifts. This indicated that compound **12** was an isomer of ambrosanoli-10,11-diol. This hypothesis was confirmed by HMBC (Fig. 2) correlations of **12** combined with sequential ^{1}H-^{1}H COSY cross-peaks. According to the ROESY data (Fig. 4), the relative configuration of compound **12** was determined. Thus the structure of compound **12** parvidiol A was assigned as shown.

The known compounds are stemanthrene A-C (**13–15**) (Kostecki et al., 2004), racemosol (**16**) (Sekine et al., 1997), 9,10-dihydro-1,5,6-trimethoxy-2,7-phenanthrenediol (**17**) (Chang et al., 2015), stilbostenin E (**18**) (Pacher et al., 2002), stilbostemin G (**19**) (Kostecki et al., 2004), (−)-3,3′-bisdemethylpinoresinol (**20**) (Kamiya et al., 2004), (+)-eudesmin (**21**) (Seo, 2010), syringaresinol (**22**) (Lodhi et al., 2008), wampetin (**23**) (Khan et al., 1983; Shen et al., 2014), 9-(isopentyloxy)-7*H*-furo [3,2-*g*] chromen-7-one (**24**) (Kalidhar, 1990), oxypeucedanin hydrate (**25**) (Lodhi et al., 2008), 3*β*-stigmasta-5,11-dien-3-ol (**26**) (Yang et al., 2008), (3*β*,5*α*,6*β*)-stigmast-7-ene-3,5,6-triol (**27**) (Piccialli and Sica, 1987), iso-lyohebecarpiin A (**28**) (Miyase et al., 1987; Wang et al., 2001), 4-hydroxy-benzenepropanol-*α*-benzoate (**29**) (Athikomkulchai et al., 2006), 3-phenylpropyl 3,4-dihydroxybenzoate (**30**) (LeBlanc et al., 2012), 4-hydroxy-3-(4-hydroxy-3,5-dimethoxyphenyl)propyl benzoic acid ester (**31**) (Renders et al., 2016), (*E*)-4-hydroxycinnamic acid methyl ester (**32**) (Speranza et al., 1988), (*E*)-ferulic acid methyl ester (**33**) (Bazin et al., 2008), and (2*E*)-3-(4-methoxyphenyl)-2-propenoic acid ethyl ester (**34**) (Concellon et al., 2005). All the known compounds were verified by comparing their spectroscopic data with those reported in the literature.

Table 2
^{1}H (500 MHz) and ^{13}C NMR (125 MHz) data of 7–10 (in $CDCl_3$).

No.	7		8		No.	9		10	
	δ_H mult. (*J* in Hz)	δ_C	δ_H mult. (*J* in Hz)	δ_C		δ_H mult. (*J* in Hz)	δ_C	δ_H mult. (*J* in Hz)	δ_C
1		135.1 s		134.8 s	**1**		160.5 s		133.3 s
2		145.3 s		145.3 s	**2**	6.39 d (9.6)	114.7 d	7.21 d (8.0)	128.4 d
3		149.1 s		149.1 s	**3**	7.78 d (9.6)	144.3 d	6.85 d (8.0)	115.4 d
4	6.86 dd (8.0, 1.4)	113.8 d	6.88 dd (8.0, 1.0)	114.0 d	**4**	7.38 s	113.2 d		156.4 s
5	6.99 dd (8.0, 7.6)	125.0 d	7.00 dd (8.0, 7.7)	125.1 d	**5**		125.9 s	6.85 d (8.0)	115.4 d
6	6.81 dd (7.6, 1.4)	121.4 d	6.83 dd (7.7, 1.0)	121.5 d	**6**		148.6 s	7.21 d (8.0)	128.4 d
1'		140.7 s		152.9 s	**7**		131.7 s	4.29 m	80.4 d
2'		113.3 s		130.6 s	**8**		143.9 s	2.28 m 2.09 m	37.1 t
3'		152.0 s		187.0 s	**9**		116.5 s	4.45 m 4.32 m	62.1 t
4'	6.33 s	97.1 d	5.54 s	99.5 d	**10**	6.83 d (2.2)	106.7 d		
5'		156.3 s		175.2 s	**11**	7.71 d (2.2)	146.6 d		
6'		116.9 s		71.7 s	**1'**	5.62 dd (7.2, 14.3) 5.64 dd (7.3, 14.3)	70.2 t		130.3 s
1''	2.72 m	29.7 t	2.77 m	29.3 t	**2'**	5.03 dd (7.2, 7.3)	119.8 d	8.04 d (7.8)	129.6 d
2''	2.92 m	31.5 t	2.72 m	30.1 t	**3'**		139.8 s	7.47 dd (7.4,7.8)	128.1 d
2-sub	3.81 s	61.4 q	3.86 s	61.4 q	**4'**	1.76 s	25.8 q	7.59 t (7.4)	133.0 d
5'-sub	3.79 s	56.6 q	3.83 s	56.0 q	**5'**	1.74 s	18.3 q	7.47 dd (7.4,7.8)	128.1 d
2'-sub	2.23 s	11.0 q	2.00 s	11.2 q	**6'**			8.04 d (7.8)	129.6 d
6'-sub	2.22 s	11.1 q	1.58 s	27.9 q	**7'**				166.7 s
					-OMe			3.23 s	56.5 q

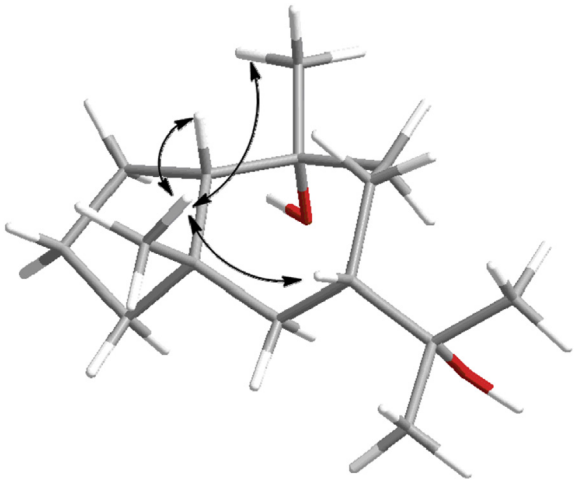

Fig. 4. Key ROESY (↔) correlations of **12**.

Table 3
Anti-nematode activity of compounds **1**, **5**, **13**, **18**, **29**, and **32**.

Compounds	IC_{50} (μM)	Compounds	IC_{50} (μM)
1	14.02 ± 0.32	**18**	2.05 ± 0.07
5	2.51 ± 0.13	**29**	4.22 ± 0.31
13	17.10 ± 0.65	**32**	1.07 ± 0.05
VC-13[a]	83.66 ± 4.33		

[a] Positive control: dichlofenthion (VC-13).

The crude extract of the non-alkaloid constituents from *S. parviflora* root had nematocidal bioactivity with RDR 76.21 ± 2.43% (at 250 μg/mL) in our study. All compounds had no cytotoxicity against the A549 cell line with IC_{50} > 500 μg/mL. Compounds **1** and **13** showed prominent killing activity against *M. incognita* (with IC_{50} values at 14.02 ± 0.32 and 17.10 ± 0.65 μM, respectively), comparable to the positive control VC-13 [dichlofenthion (Sigma-Aldrich) IC_{50} value at 83.66 ± 4.33 μM]. Furthermore, compounds **5**, **18**, **29**, and **32** showed even stronger nematocidal bioactivity (with IC_{50} values at 2.51 ± 0.13, 2.05 ± 0.07, 4.22 ± 0.31, and 1.07 ± 0.05 μM, respectively) (Table 3). The non-alkaloid fraction of a few *Stemona* species was also studied previously, showing other bioactivities in certain phenanthrenes and stilbenes (Pacher et al., 2002; Zhao et al., 1995). These data indicate that the non-alkaloid constituents in *S. parviflora* play an important defensive role against soil worms.

In conclusion, 34 compounds, including twelve undescribed ones parviphenanthrines A-F (**1–6**), parvistilbines A and B (**7** and **8**), parviesters A-C (**9–11**), and parvidiol A (**12**), were isolated from the roots of *S. parviflora*. The chemical constituents in the *S. parviflora*, ie. compounds **1**, **13**, **5**, **18**, **29**, and **32**, showed nematocidal bioactivity and no cytotoxicity in our study. According to the current systematic isolation results and the published literature, the phytochemicals isolated from the *Stemona* genus fit into different structural 11 classes [alkaloids (Suzuki, 1934), phenanthrenes (Pacher et al., 2002), stilbenes (Zhao et al., 1995), dehydrotocopherol (Brem et al., 2004), phenylpropanoids (Ge et al., 2007), sterols, anthraquinone (Yang et al., 2008), lignins, cycle esters, sesquiterpenoids, and coumarins]. Lignins, cycle esters, sesquiterpenoids, and coumarins were firstly isolated from this genus. The previous evidence of the alkaloids as the main bioactive constituents in *Stemona* species (Leung, 2006), together with the isolation of methylated phenanthrenes and stilbenes with various bioactivities, show the great potential of this herb in medicinal usage. In addition, the phenols, with better safety profile than alkaloids, may be developed as a safer nematocidal reagent in the future.

3. Experimental section

3.1. General

Optical rotations were acquired on a Cataceo Co, Ltd. Polar-L polarimeter. ECD were recorded on a Chirascan instrument. UV spectra were obtained on a Shimadzu UV-250 spectrometer. IR spectra were obtained on a Thermo Nicolet 380 spectrometer with KBr pellets. NMR spectra were measured on a Bruker AV-500 spectrometer with TMS as an internal standard. ESIMS and HRESIMS were obtained with a Waters Autospec Premier Spectrometer or Ultimate 3000-Brucker Compact. Silica gel (200–300 mesh and H, Qingdao Marine Chemical Inc., Qingdao, China), RP-18 (40–70 μm, Merck & Co Inc LiChrosorb RP-18, Kenilworth, USA) and Sephadex LH-20 (Amersham Biosciences, lippsala, Sweden) were used for column chromatography. Semi-preparative

HPLC was performed on an Agilent 1260 liquid chromatograph with a Cosmosil, C18-M-II ϕ 5 μm, 10 mm × 250 mm, column. Fractions were detected by TLC and spots were visualized by heat after soaking in 10% H_2SO_4 (in alcohol). The planar structures and 3D structures were drawn with ChemBioOffice 2010. The ECD picture was plotted with OriginPro 2010.

3.2. Plant material

The *Stemona parviflora* C. H. Wright (Stemonaceae family) roots were collected in May (dry season) 2014 from volcanic area in Haikou suburban district (E110.292342, N19.892999), Hainan Province, People's Republic of China. The plant was identified by S.-Z. H. and Dr. G. Chen (Kunming Institute of Botany, Chinese Academy of Sciences), voucher specimen (^{HUANG0010}) was deposited at the Hainan Key Laboratory for Research and Development of Natural Products from Li Folk Medicine, Institute of Tropical Bioscience and Biotechnology, Chinese Academy of Tropical Agriculture Sciences, Haikou, People's Republic of China.

3.3. Extraction and isolation

The air-dried *S. parviflora* roots (6.0 kg) were sliced and extracted with alcohol (15 L) with reflux three times, after evaporation, which was partitioned between H_2O (pH value was adjusted to 2.0 with 2 M HCl) and ethyl acetate. After evaporated of the ethyl acetate part the residue (87 g) was chromatographed on silica gel with petroleum ether - ethyl acetate (20:0 to 0:1, v/v) to give eight fractions. Fraction 2 (2.8 g) was chromatographed on silica gel (petroleum ether -Me_2CO, 5:1, v/v), RP-18 (H_2O-MeOH, 1:9 to 0:1, v/v) and Sephadex LH-20 ($CHCl_3$-MeOH, 1:1, v/v) columns to yield compounds **9** (6.9 mg), **11** (47.1 mg), **23** (14.5 mg), and **24** (6.8 mg). Fraction 3 (3.7 g) was chromatographed on silica gel (petroleum ether-Me_2CO, 5:1, v/v), silica gel (petroleum ether-Me_2CO, 4:1, v/v), RP-18 (H_2O-MeOH, 1:9 to 0:1, v/v) to yield compounds **6** (20.5 mg), **14** (34.5 mg), and **26** (24.4 mg), and semi-preparative HPLC (MeOH-H_2O, 30:70, v/v) to yield compounds **1** (9.8 mg) and **2** (4.7 mg). Fraction 4 (6.9 g) was separated by silica gel (petroleum ether-Me_2CO, 3:1, v/v), RP-18 (H_2O-MeOH, 1:9 to 0:1, v/v), and semi-preparative HPLC (MeOH/H_2O, 35:65, v/v) to yield compounds **4** (14.3 mg), **21** (13.5 mg), and **27** (14.6 mg). Fraction 5 (10.5 g) was chromatographed on silica gel (petroleum ether -Me_2CO, 4:1, v/v) to yield compound **15** (143 mg) and fractions 5a and 5b. Fraction 5a was chromatographed sequentially on RP-18 (H_2O-MeOH, 1:9 to 0:1, v/v) and Sephadex LH-20 ($CHCl_3$-MeOH, 1:1, v/v) columns to yield compounds **3** (6.7 mg), **5** (37.8 mg), and **12** (4.8 mg). Fraction 2b was separated using silica gel (petroleum ether-Me_2CO, 3:1, v/v), RP-18 (H_2O-MeOH, 1:9 to 0:1, v/v) and semi-preparative HPLC (MeOH-H_2O, 35:65, v/v) to yield compounds **18** (21.3 mg) and **25** (7.6 mg). Fraction 6 (16.4 g) was chromatographed on silica gel (petroleum ether -Me_2CO, 3:1, v/v) to yield compound **13** (231 mg) and fractions 6a and 6b. Fraction 6a was chromatographed sequentially on RP-18 (H_2O-MeOH, 1:9 to 0:1, v/v) and Sephadex LH-20 ($CHCl_3$-MeOH, 1:1, v/v) columns to yield compounds **7** (17.9 mg), **19** (38.9 mg), and **24** (4.1 mg). Fraction 6b was separated using silica gel (petroleum ether-Me_2CO, 2:1, v/v), RP-18 (H_2O-MeOH, 1:9 to 0:1, v/v) to yield compounds **16** (52.3 mg). Fraction 7 (11.6 g) was chromatographed on silica gel (petroleum ether -Me_2CO, 4:1, v/v) to fractions 7a, 7b, and 7c. Fraction 7a was chromatographed sequentially on RP-18 (H_2O-MeOH, 1:9 to 0:1, v/v) and Sephadex LH-20 ($CHCl_3$-MeOH, 1:1, v/v) columns to yield compounds **8** (7.7 mg) and **20** (32.6 mg). Fraction 7b was separated using silica gel (petroleum ether-Me_2CO, 2:1, v/v), RP-18 (H_2O-MeOH, 1:9 to 0:1, v/v) and semi-preparative HPLC (MeOH-H_2O, 40:60, v/v) to yield compounds **22** (15.7 mg) and **31** (17.2 mg). Fraction 7c was chromatographed in turn, on RP-18 (H_2O-MeOH, 1:9 to 0:1, v/v) and Sephadex LH-20 ($CHCl_3$-MeOH, 1:1, v/v) columns to yield compounds **33** (21.9 mg). Fraction 8 (21.2 g) was chromatographed on silica gel (petroleum ether -Me_2CO, 2:1, v/v) to yield fractions 8a and 8b. Fraction 8a was chromatographed sequentially on RP-18 (H_2O-MeOH, 1:9 to 0:1, v/v) and Sephadex LH-20 ($CHCl_3$-MeOH, 1:1, v/v) columns to yield compounds **32** (11.2 mg) and **34** (22.2 mg). Fraction 8b was separated using silica gel (petroleum ether-Me_2CO, 1:1, v/v), RP-18 (H_2O-MeOH, 1:9 to 0:1, v/v) and semi-preparative HPLC (MeOH-H_2O, 50:50, v/v) to yield compounds **10** (2.3 mg), **29** (6.5 mg), and **30** (11.8 mg).

3.3.1. Parviphenanthrine A (1)

White crystal; mp. 108.9–109.5 °C, $[\alpha]_D^{25}$ −20.7 (*c* 0.14, MeOH); UV (MeOH) λ_{max} (logε) 213 (5.36), 310 (4.44), 201 (5.72) nm; IR (KBr) ν_{max} 3416, 2924, 2851, 1662, 1573, 1484, 1448, 1426, 1396, 1298, 1157, 1106, 856 cm^{-1}; ECD (*c* 0.07 mM, MeOH), λ_{max} ($\Delta\varepsilon$) 217 (+2.00), 262 (−1.06), 250 (−2.22), 288 (+0.84), 347(-2.26), 400 (−1.21) nm; ^1H and ^{13}C NMR data see Table 1; ESIMS positive *m/z* $[M+Na]^+$ 309 (100); HRESIMS *m/z* $[M+Na]^+$ 309.1105 (calcd for $C_{17}H_{18}O_4Na$, 309.1103).

3.3.2. Parviphenanthrine B (2)

Colorless solid; mp. 136.2–138.2 °C, UV (MeOH) λ_{max} (logε) 280 (5.35), 295 (5.19), 311 (4.90) nm; IR (KBr) ν_{max} 3384, 2995, 2922, 1698, 1642, 1549, 1415, 1370, 1288, 1235, 1090, 985 cm^{-1}; ^1H and ^{13}C NMR data see Table 1 . ESIMS positive *m/z* $[M+Na]^+$ 321 (100); HRESIMS *m/z* $[M-H]^-$ 297.0771 (calcd for $C_{17}H_{13}O_5$, 297.0763).

3.3.3. Parviphenanthrine C (3)

Colorless solid; mp. 144.7–146.2 °C, UV (MeOH) λ_{max} (logε) 280 (5.17) nm; IR (KBr) ν_{max} 3447, 1642, 1420, 1317, 1292, 1161, 1072, 989 cm^{-1}; ^1H and ^{13}C NMR data see Table 1; ESIMS positive *m/z* $[M+Na]^+$ 295 (100); HRESIMS *m/z* $[M-H]^-$ 271.0976 (calcd for $C_{16}H_{15}O_4$, 271.0970).

3.3.4. Parviphenanthrine D (4)

White crystal; m.p. 147.3–148.5 °C; UV (MeOH) λ_{max} (logε) 282 (4.19), 297 (4.07) nm; IR (KBr) ν_{max} 3419, 2996, 2926, 2834, 1715, 1606, 1491, 1464, 1402, 1391, 1275, 1138, 1117 cm^{-1}; ^1H and ^{13}C NMR data see Table 1; ESIMS positive *m/z* $[M+Na]^+$ 323 (100); HRESIMS *m/z* $[M+Na]^+$ 323.1255 (calcd for $C_{18}H_{20}O_4Na$, 323.1254).

3.3.5. Parviphenanthrine E (5)

Colorless solid; mp. 141.5–143.2 °C, UV (MeOH) λ_{max} (logε) 311(4.90), 295(5.19), 280 (5.28)nm; IR (KBr) ν_{max} 3459, 2959, 2839, 1606, 1475, 1414, 1319, 1282, 1214, 1155, 1077, 1065, 999, 824 cm^{-1}; ^1H and ^{13}C NMR data see Table 1; ESIMS positive *m/z* $[M+Na]^+$ 309 (100); HRESIMS *m/z* $[M+Na]^+$ 309.1098 (calcd for $C_{17}H_{18}O_4Na$, 309.1103).

3.3.6. Parviphenanthrine F (6)

Colorless solid; mp. 138.9–143.1 °C, UV (MeOH) λ_{max} (logε) 282 (5.28) nm; IR (KBr) ν_{max} 3450, 1641, 1563, 1414, 1089, 539 cm^{-1}; ^1H and ^{13}C NMR data see Table 1; ESIMS negative *m/z* $[M-H]^-$ 313 (100); HRESIMS *m/z* $[M-H]^-$ 313.1446 (calcd for $C_{19}H_{21}O_4$, 313.1445).

3.3.7. Parvistilbine A (7)

White solid; mp. 115.4–117.3 °C, UV (MeOH) λ_{max} (logε) 280 (4.64), 224 (5.29) nm; IR (KBr) ν_{max} 3470, 2931, 1700, 1597, 1495, 1471, 1445, 1310, 1288, 1119, 1077, 1001, 752 cm^{-1}; ^1H and ^{13}C NMR data see Table . ESIMS positive *m/z* $[M+Na]^+$ 325 (100); HRESIMS *m/z* $[M+Na]^+$ 325.1409 (calcd for $C_{18}H_{22}O_4Na$, 325.1416).

3.3.8. Parvistilbine B (8)

Colorless solid; mp. 114.2–116.3 °C, $[\alpha]_D^{26}$ −21.4 (*c* 0.07, MeOH); UV (MeOH) λ_{max} (logε) 240 (4.13), 279 (3.79), 297 (3.67) nm; IR (KBr) ν_{max} 3392, 2932, 2851, 1710, 1655, 1609, 1471, 1387, 1371, 1219, 1177, 1089, 998, 840, 755 cm^{-1}; ^1H and ^{13}C NMR data see Table 2;

ESIMS positive *m/z* $[M+Na]^+$ 341 (100); HRESIMS *m/z* $[M+Na]^+$ 341.1358 (calcd for $C_{18}H_{22}O_5Na$, 341.1359).

3.3.9. Parviester A (9)

Colorless solid; mp. 278.4–181.8 °C, UV (MeOH) λ_{max} (logε) 216 (5.29), 248 (5.18), 300 (4.89) nm; IR (KBr) ν_{max} 3450, 1642, 1565, 1410, 1069 cm^{-1}; ^1H and ^{13}C NMR data see Table 2; ESIMS positive *m/z* $[M+Na]^+$ 563 (100); HRESIMS *m/z* $[M+Na]^+$ 563.1676 (calcd for $C_{32}H_{28}O_8Na$, 563.1682).

3.3.10. Parviester B (10)

Colorless solid; mp. 126.2–128.2 °C, $[\alpha]_D^{25}$ −3.75 (*c* 0.08, MeOH); UV (MeOH) λ_{max} (logε) 274 (5.32), 226 (5.56) nm; IR (KBr) ν_{max} 3445, 1715, 1694, 1643, 1515, 1453, 1412, 1278, 1093, 1072, 835, 712 cm^{-1}; ^1H and ^{13}C NMR data see Table 2; ESIMS positive *m/z* $[M+Na]^+$ 309 (100); HRESIMS *m/z* $[M+Na]^+$ 309.1102 (calcd for $C_{17}H_{18}O_4Na$, 309.1103).

3.3.11. Parviester C (11)

Colorless oil; $[\alpha]_D^{28}$ −0.33 (c 0.06, MeOH); UV (MeOH) λ_{max} (logε) 230 (5.58) nm; IR (KBr) ν_{max} 3444, 1640, 1561, 1412, 1064, 988 cm^{-1}; ^1H NMR (500 MHz, $CDCl_3$) δ: 1.64 (s, 3H, H-4), 4.53 (m, 2H, H-5), 3.86 (s, 3H, -OMe); ^{13}C NMR (125 MHz, $CDCl_3$) δ: 175.5 (s, C-1), 98.1 (s, C-2), 172.7 (s, C-3), 6.8 (q, C-4), 65.6 (s, C-5), 57.8 (q, -OMe); ESIMS negative *m/z* $[M-H]^-$ 319 (100); HRESIMS *m/z* $[M-H]^-$ 319.0671 (calcd for $C_{12}H_{15}O_{10}$, 319.0665).

3.3.12. Parvidiol A (12)

Colorless oil; $[\alpha]_D^{25}$ +3.68 (*c* 0.095, MeOH); UV (MeOH) λ_{max} (logε) 202 (4.20), 207 (4.17), 224 (3.93) nm; IR (KBr) ν_{max} 3130, 2963, 2960, 1647, 1561, 1408, 1379, 1087 cm^{-1}; ^1H NMR (500 MHz, $CDCl_3$) δ: 1.67 (dd, J = 13.4, 3.2 Hz, 1H, H-1), 2.06 (m, 1H, H-2), 1.46 (m, 1H, H-2), 1.74 (m, 1H, H-3), 1.54 (m, 1H, H-3), 1.76 (m, 1H, H-4), 1.50 (m, 1H, H-4), 1.38 (m, 1H, H-6), 1.20 (m, 1H, H-6), 1.70 (m, 1H, H-7), 1.42 (m, 1H, H-8), 1.21 (m, 1H, H-8), 1.80 (m, 1H, H-9), 1.11 (m, 1H, H-9), 1.31 (s, 3H, H-12), 1.30 (s, 3H, H-13), 1.13 (s, 3H, H-14), 0.93 (s, 3H, H-15); ^{13}C NMR (125 MHz, $CDCl_3$) δ: 49.4 (d, C-1), 20.3 (t, C-2), 20.9 (t, C-3), 41.8 (t, C-4), 34.3 (s, C-5), 41.7 (t, C-6), 42.0 (d, C-7), 21.2 (t, C-8), 43.7 (t, C-9), 72.6 (s, C-10), 74.8 (s, C-11), 29.5 (q, C-12), 29.9 (q, C-13), 18.9 (q, C-14), 22.1(q, C-15); ESIMS positive *m/z* $[M+Na]^+$ 263 (100); HREIMS *m/z* $[M+Na]^+$ 263.1980 (calcd for $C_{15}H_{28}O_2Na$, 263.1987).

3.4. Cytotoxicity assay

The cytotoxicity assay against the A549 cell line (IC_{50}) was carried out using the MTT methods as described earlier (Huang et al., 2015). If the compound at maximum concentration (500 μg/mL) showed lower than 50% death rate, IC_{50} was marked with > 500 μg/mL.

3.5. Antinematode bioassay

According to Baermann-funnel method juveniles of *Meloidogyne incognita* were collected from the infected *Aquilaria sinesis* roots (Zhuo et al., 2015). The anti-nematodes activities of all the compounds (25 mg/mL) were tested using the method reported in the literature (Zhuo et al., 2015). The dimethyl sulfoxide (DMSO) and dichlofenthion (VC-13) was established as negative and positive control, respectively. The activity (NA) was assessed by counting the dead nematodes (n > 100) under a microscope after incubation at 28 °C for 24 h. According the formula: NA = DN/SN × 100% (DN: number of dead nematodes, SN: sum of all counted nematodes, SN > 100), the NA value was calculated. Using the formula: RDR = NA_n—NA_0(NA_n: nematocidal activity of compounds, NA_0 nematocidal activity of blank control), the relative death rate (RDR) was calculated (Zhuo et al., 2015). If the RDR of any compounds exceeded 80%, their IC_{50} was assayed and calculated by the Reed and Muench method (Reed and Muench, 1938).

Acknowledgments

This work was supported by the grant from China Agriculture Research System (CARS-21), Financial Fund of the Ministry of Agriculture and Rural Affairs, P. R. of China (NFZX2018), and Central Public-interest Scientific Institution Basal Research Fund for Chinese Academy of Tropical Agricultural Sciences (17CXTD-15, 1630052016008). The authors thank Dr. Y. L. Huang (Dept. of Clinical Development. Pfizer China Research and Development Co. Ltd, Shanghai) for initial proofreading of this paper.

Appendix A. Supplementary data

Supplementary data related to this article can be found at https://doi.org/10.1016/j.phytochem.2018.12.021.

References

Athikomkulchai, S., Prawat, H., Thasana, N., Ruangrungsi, N., Ruchirawat, S., 2006. COX-1, COX-2 inhibitors and antifungal agents from *Croton hutchinsonianus*. Chem. Pharm. Bull. 54, 262–264.

Bazin, M.A., El Kihel, L., Jouanne, M., Lancelot, J.C., Rault, S., 2008. Synthesis of new avenalumic carboxamide derivatives in the ferulic series. Synth. Commun. 38, 3947–3959.

Bird, D.M., Kaloshian, I., 2003. Are roots special? Nematodes have their say. Physiol. Mol. Plant Pathol. 62, 115–123.

Brem, B., Seger, C., Pacher, T., Hartl, M., Hadacek, F., Hofer, O., Vajrodaya, S., Greger, H., 2004. Antioxidant dehydrotocopherols as a new chemical character of *Stemona* species. Phytochemistry 65, 2719–2729.

Chang, C., Hsu, Y., Lee, C., Wu, C., Wu, Y., Chuang, T., 2015. Isolation and cytotoxicity evaluation of the chemical constituents from *Cephalantheropsis gracilis*. Int. J. Mol. Sci. 16, 3980–3989.

Commission of China Pharmacopoeia, 2015. Pharmacopoeia of the People's Republic of China, vol. 1. China Medical Science and Technology Press, Beijing, pp. 132.

Concellon, J.M., Concellon, C., Mejica, C., 2005. An easy, efficient, and completely stereoselective synthesis of (E)-α,β-unsaturated esters via sequential aldol-type/elimination reactions promoted by samarium diiodide or chromium dichloride. J. Org. Chem. 70, 6111–6113.

Dai, H., 2010. Records of Li Folk Medicine, vol. 2. China Science and Technology Press, Beijing, pp. 252.

Ge, F., Ke, C., Tang, W., Yang, X., Tang, C., Qin, G., Xu, R., Li, T., Chen, X., Zuo, J., Ye, Y., 2007. Isolation of chlorogenic acids and their derivatives from Stemona japonica by preparative HPLC and evaluation of their anti-AIV (H5N1) activity in vitro. Phytochem. Anal. 18, 213–218.

Huang, S.Z., Kong, F.D., Ma, Q.Y., Guo, Z.K., Zhou, L.M., Wang, Q., Dai, H.F., Zhao, Y.X., 2016. Nematocidal Stemona alkaloids from *Stemona parviflora*. J. Nat. Prod. 79, 2599–2605.

Huang, S.Z., Zhang, X., Ma, Q.Y., Zheng, Y.T., Dai, H.F., Wang, Q., Zhou, J., Zhao, Y.X., 2015. Anti-HIV terpenoids from *Daphne aurantiaca* Diels. stems. RSC Adv. 5, 80254–80263.

Kalidhar, S.B., 1990. A distinction between 5-alkoxy- and 8-alkoxyfuro[3',2':6,7]coumarins using proton NMR alkoxylation shifts. Indian J. Chem. B. 29B, 980–983.

Kamiya, K., Tanaka, Y., Endang, H., Umar, M., Satake, T., 2004. Chemical constituents of *Morinda citrifolia* fruits inhibit copper-induced low-density lipoprotein oxidation. J. Agric. Food Chem. 52, 5843–5848.

Khan, N.U., Naqvi, S.W.I., Ishratullah, K., 1983. Wampetin, a furocoumarin from *Clausena wampi*. Phytochemistry 22, 2624–2625.

Kostecki, K., Engelmeier, D., Pacher, T., Hofer, O., Vajrodaya, S., Greger, H., 2004. Dihydrophenanthrenes and other antifungal stilbenoids from *Stemona* cf. *pierrei*. Phytochemistry 65, 99–106.

LeBlanc, L.M., Pare, A.F., Jean-Francois, J., Hebert, M.J.G., Surette, M.E., Touaibia, M., 2012. Synthesis and antiradical/antioxidant activities of caffeic acid phenethyl ester and its related propionic, acetic and benzoic acid analogs. Molecules 17, 14637–14650.

Leung, P.H.H., 2006. Chemical, Pharmacological and Intestinal Absorption Studies of *Stemona* Alkaloids from Radix Stemonae. pp. 200.

Lodhi, M.A., Choudhary, M.I., Malik, A., Ahmad, S., 2008. α-Chymotrypsin inhibition studies on the lignans from *Vitex negundo* Linn. J. Enzym. Inhib. Med. Chem. 23, 400–405.

Miyase, T., Ueno, A., Takizawa, N., Kobayashi, H., Oguchi, H., 1987. Studies on the glycosides of *Epimedium grandiflorum* Morr. Var. *thunbergianum* (Miq.) Nakai. II. Chem. Pharm. Bull. 35, 3713–3719.

Ngan, N.T.T., Quang, T.H., Tai, B.H., Song, S.B., Lee, D., Kim, Y.H., 2012. Anti-inflammatory and PPAR transactivational effects of components from the stem bark of *Ginkgo biloba*. J. Agric. Food Chem. 60, 2815–2824.

Oka, Y., Shuker, S., Tkachi, N., 2009. Nematicidal efficacy of MCW-2, a new nematicide of the fluoroalkenyl group, against the root-knot nematode *Meloidogyne javanica*. Pest Manag. Sci. 65, 1082–1089.

Pacher, T., Seger, C., Engelmeier, D., Vajrodaya, S., Hofer, O., Greger, H., 2002. Antifungal stilbenoids from *Stemona collinsae*. J. Nat. Prod. 65, 820–827.
Piccialli, V., Sica, D., 1987. Four new trihydroxylated sterols from the sponge *Spongionella gracilis*. J. Nat. Prod. 50, 915–920.
Reed, L.J., Muench, H., 1938. A simple method for estimating fifty percent endpoints. Am. J. Hyg. 27, 493–497.
Renders, T., Schutyser, W., Van den Bosch, S., Koelewijn, S.-F., Vangeel, T., Courtin, C.M., Sels, B.F., 2016. Influence of acidic (H3PO4) and alkaline (NaOH) additives on the catalytic reductive fractionation of lignocellulose. ACS Catal. 6, 2055–2066.
Sekine, T., Fukasawa, N., Murakoshi, I., Ruangrungsi, N., 1997. A 9,10-dihydrophenanthrene from *Asparagus racemosus*. Phytochemistry 44, 763–764.
Seo, Y., 2010. Antioxidant activity of the chemical constituents from the flower buds of *Magnolia denudata*. Biotechnol. Bioproc. Eng. 15, 400–406.
Shen, D., Chan, Y., Hwang, T., Juang, S., Huang, S., Kuo, P., Thang, T.D., Lee, E.J., Damu, A.G., Wu, T., 2014. Constituents of the roots of *Clausena lansium* and their potential anti-inflammatory activity. J. Nat. Prod. 77, 1215–1223.
Speranza, G., Martignoni, A., Manitto, P., 1988. Studies on aloe. Part 5. Iso-aleoresin A, a minor constituent of Cape aloe. J. Nat. Prod. 51, 588–590.
Stephens, P.J., Pan, J.J., Krohn, K., 2007. Determination of the absolute configurations of pharmacological natural products via density functional theory calculations of vibrational circular dichroism: the new cytotoxic iridoid prismatomerin. J. Org. Chem. 72, 7641–7649.
Suzuki, K., 1934. Alkaloids of Stemona IV. Stemonidine and its derivative from *Stemona japonica* Miq. Yakugaku Zasshi 54, 561–566 Abstracts 101-104.
Vieira, I.J.C., Figueiredo, E.R., Freitas, V.R., Mathias, L., Braz-Filho, R., Araujo, R.M., 2010. A new sesquiterpene from *Trichilia casareti* (Meliaceae). Am. J. Anal. Chem. 1, 70–72.
Wang, C., Liu, Y., Li, C., Chen, S., Qin, G., 2001. Study of chemical constituents from *Lyonia ovalifolia* var *hebecarpa*. J. Henan Med. Univ. 36, 743–745.
Xing, F., Chen, H., Qin, X., Zhang, R., Zhou, J., 2014. Illustrated Hand Book of Plants in Tropical Rainforest Area of China, vol. 3. Huazhong University of Science & Technology Press, Wuhan China, pp. 1156.
Yang, X., Tang, C., Ke, C., Ye, Y., 2008. Chemical constituents of *Stemona japonica*. Nat. Prod. Res. Dev. 20, 399–402.
Yu, S.H., 1999. Plant disease complexes involving pathogenic nematodes. Acta Phytopathol. Sin. 29, 1–7.
Zhao, W., Qin, G., Ye, Y., Xu, R., Le, X., 1995. Bibenzyls from *Stemona tuberosa*. Phytochemistry 38, 711–713.
Zhuo, H.S., Ni, H.H., Yun, M.Q., He, M.M., Liang, Z.M., Fu, D.H., Ping, J.Y., Hai, W.Q., Xing, Z.Y., 2015. The phytochemicals with antagonistic activities toward pathogens of a disease complex caused by *Meloidogyne incognita* and *Ralstonia solanacearum*. J. Pure Appl. Microbiol. 9, 209–213.